

Spectroscopy of excited states in ^{102}Mo and ^{106}Ru

J. Koenig, H. Bohn, T. Faestermann, P. Kienle, H. J. Körner,
W. A. Mayer, D. Pereira, K. E. Rehm, and H. J. Scheerer
*Physik-Department, Technische Universität München, D-8046 Garching,
Federal Republic of Germany*

(Received 9 June 1981)

Excited states in the transitional nuclei ^{102}Mo and ^{106}Ru have been populated in ^{18}O induced two neutron transfer reactions at bombarding energies around 5 MeV/nucleon. The succeeding γ decay was measured employing a particle- γ coincidence technique in which the ejectiles were identified with a quadrupole-three-dipole magnetic spectrograph. This method is especially suited for studying the decay modes of regions with selected excitation energy and spin. A characteristic evolution in the population of known states ($I^\pi \leq 4^+$) with changing excitation energy was observed. Previously unknown γ transitions are attributed to the decay of 6^+ and 8^+ yrast states in ^{102}Mo and ^{106}Ru , respectively.

NUCLEAR REACTIONS $^{100}\text{Mo} (^{18}\text{O}, ^{16}\text{O})$, $E_{\text{lab}}(^{18}\text{O}) = 84$ MeV, $\theta_{\text{lab}} = 34^\circ$; $^{104}\text{Ru} (^{18}\text{O}, ^{16}\text{O})$, $E_{\text{lab}}(^{18}\text{O}) = 84$ and 100 MeV, $\theta_{\text{lab}} = 34^\circ$ and 30° . Measured particle- γ coinc. for selected excitation energy ranges, deduced ^{102}Mo and ^{106}Ru level energies (and spins). Enriched targets.

I. INTRODUCTION

Much of the existing spectroscopic information about excited states in β^- -unstable neutron rich even Mo and Ru nuclei was obtained from γ -ray spectroscopy following fission. Both γ decay of primary fission fragments¹ and that following β^- decay of fission products separated by fast chemical procedures^{2,3} were studied. Mainly low spin states are located in these experiments. This is also true for (t,p) reactions,^{4,5} where primarily 0^+ and 2^+ states are excited.

Heavy ion induced transfer reactions offer another possibility to populate excited states in neutron rich nuclei. It was shown⁶ that $(^{18}\text{O}, ^{16}\text{O})$ reactions at bombarding energies close to the Coulomb barrier can successfully be applied to study excited states with $I^\pi \leq 4^+$ in neutron rich $A \approx 100$ nuclei.

The present work reports on particle- γ coincidence experiments employing the $(^{18}\text{O}, ^{16}\text{O})$ reaction on neutron rich targets at incident energies well above ($> 50\%$) the Coulomb barrier in order to investigate the possibility to locate high spin states in the heavy final nuclei. At bombarding energies above the barrier many channels contribute to the total reaction cross section. Therefore, a

particle detector with both good channel resolution and large solid angle is necessary for coincidence experiments with high resolution Ge(Li) detectors. These requirements are met by detecting the outgoing particles with a quadrupole-three-dipole (Q3D) magnetic spectrograph with a solid angle of 11 msr. The experimental method is outlined in Sec. II and details are given in Sec. III. The results are presented in Sec. IV and are discussed in Sec. V.

II. EXPERIMENTAL METHOD

In $(^{18}\text{O}, ^{16}\text{O})$ reactions on heavy target nuclei most of the strength is located in a rather narrow band of Q values. This Q window corresponds to excitation energies of several MeV in the heavy final nucleus. Its centroid and width depends in detail on the kinematical conditions involved in the reaction.^{7,8}

To illustrate the basic features, Fig. 1 schematically shows the location of strength calculated for the reaction $^{104}\text{Ru}(^{18}\text{O}, ^{16}\text{O})^{106}\text{Ru}$ at 84 MeV incident energy for several values of the transferred angular momentum L . The Q window is plotted with respect to the yrast line of ^{106}Ru in an excitation energy (E^*) vs spin (I) plane. Reaction Q

values were converted into excitation energies of ^{106}Ru by assuming that the outgoing ^{16}O particles are produced in their ground states. The yrast line was parametrized using a rigid body moment of inertia with $r_0=1.2$ fm, arbitrarily reduced by $\sim 20\%$ in order to approximately fit the positions of known³ yrast states with $I^\pi \leq 4^+$. These states together with other known³ levels are indicated in Fig. 1 by the short horizontal bars. The solid dots together with the vertical bars represent the centroids and the widths (FWHM) of the Gaussian-type optimum Q -value distributions, predicted for L values of 0, 2, 4, 6, and 8 \hbar by DWBA calculations with the full finite range code PTOLEMY.⁹ A one step cluster transfer of an $S=0$ neutron pair was assumed using the bound state parameters $r_0=1.25$ fm, $a=0.65$ fm for ^{18}O and ^{106}Ru . The optical potential parameters for the incoming and outgoing channels were taken from fits to elastic scattering data from neighboring systems.¹⁰

It can be seen from Fig. 1 that due to the positive ground state Q value of $+2.184$ MeV a region of high level density is populated strongly already for $L=0$ transfer. With increasing L the predicted

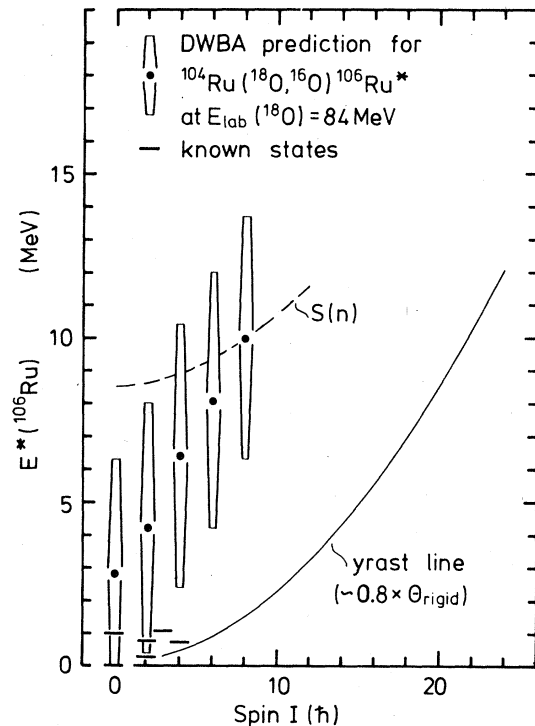


FIG. 1. Centroids (solid dots) and widths (FWHM, vertical bars) of optimum angular momentum ($L=0, 2, \dots, 8 \hbar$) transfer strengths calculated for the reaction $^{104}\text{Ru}(^{18}\text{O}, ^{16}\text{O})^{106}\text{Ru}$ at 84 MeV bombarding energy (see text).

location of the optimum probability for transferring a given L value to ^{106}Ru is shifted linearly to higher excitation energies. Utilizing the magnetic spectrograph as a Q -value selector, the investigation of regions differing in spin composition becomes possible by selecting different excitation energy bins (as deduced from Q -value bins) in the position ($B \cdot \rho$) spectrum. With particle- γ coincidence experiments the γ decay originating exclusively from levels initially populated within such selected regions can be studied. Since the deexcitation γ -ray flux is finally collected by states near to the yrast line, γ transitions between the higher spin members of the yrast states are enhanced by selecting higher excitation energy ranges. At excitation energies above the one neutron binding energy, neutron emission out of the heavy final nucleus is expected to occur. For the present case the γ -ray spectrum coincident with ^{16}O ejectiles will become dominated by γ transitions between states located in ^{105}Ru if the excitation energy window is moved across the line, where $\Gamma_\gamma \approx \Gamma_n$ in ^{106}Ru (dashed line in Fig. 1). Depending on how much of the reaction strength for higher L values is concentrated above this line, spectroscopy of higher spin states in the "daughter" nucleus will be feasible. By shifting the excitation energy window to still higher excitation energies two neutron emission processes may be investigated.

III. EXPERIMENTAL DETAILS

Particle- γ coincidence experiments were performed by bombarding highly enriched ^{100}Mo and ^{104}Ru targets with ^{18}O beams from the Munich MP tandem accelerator. The experimental details are summarized in Table I. The targets were mounted in the center of the scattering chamber of the Munich Q3D magnetic spectrograph. The beam spot size on the target was about 1 mm (within the reaction plane) \times 3 mm (vertically). The outgoing particles were momentum analyzed by the magnetic spectrograph and identified in a 1 m long position sensitive ΔE - E ionization chamber¹¹ mounted in the focal plane. The particle momentum range covered by the ionization chamber was 5.9%, corresponding to an excitation energy range of ~ 8.5 MeV. The energy resolution as obtained from the position spectrum was ~ 500 keV due to the thick targets used. For each bombarding energy the angle of the spectrograph (see Table I) was chosen to be close to the grazing angle as deduced from ^{18}O induced reactions on neighboring nuclei.^{7,12} The entrance slits of the spectrograph were

opened to accept a solid angle of 11 msr, corresponding to an angular range of $\pm 3.5^\circ$ (lab). Gamma rays from the decay of excited reaction products were detected in a true-coaxial Ge(Li) detector with an active volume of 130 cm³, located at 90° to the beam axis at a distance of 3.0 cm from the target. Thus, an acceptance angular range of 51°–129° was covered by the Ge(Li) detector. The incident beam was stopped in a well shielded Faraday cup. Gamma rays originating from the cup produced a negligible counting rate in the Ge(Li) detector. The rate in the Ge(Li) detector resulting from the target was kept at ~ 30 kHz, equivalent to beam currents of the order of 1 particle nA. As an example for the particle resolution achieved with the Q3D magnetic spectrograph, Fig. 2(a) shows a two-dimensional ΔE vs E_{total} contour plot for the reaction $^{18}\text{O} + ^{104}\text{Ru}$. Ejectile groups ranging from Be to F are observed and are clearly resolved. Figure 2(b) shows the corresponding γ -ray spectrum coincident with all particles shown in Fig. 2(a). This γ -ray spectrum is quite complex due to the many contributing reaction channels. Selecting the ^{16}O exit channel, the insert of Fig. 2(b) shows the time spectrum of all ^{16}O - γ coincidences. The time resolution (FWHM) was about 80 nsec, mainly limited by the spread in charge collection time due to the finite vertical opening of the ionization chamber. (The contribution due to flight time differences of ^{16}O ions is estimated to be 20 nsec.) From this time spectrum the excellent ratio of true to random coincidences is evident. In the following the discussion is concentrated on the two neutron transfer reaction (^{18}O , ^{16}O), leading to the final nuclei ^{102}Mo and ^{106}Ru , respectively.

IV. EXPERIMENTAL RESULTS

All γ -ray spectra displayed in the following were obtained by setting appropriate gates on the respec-

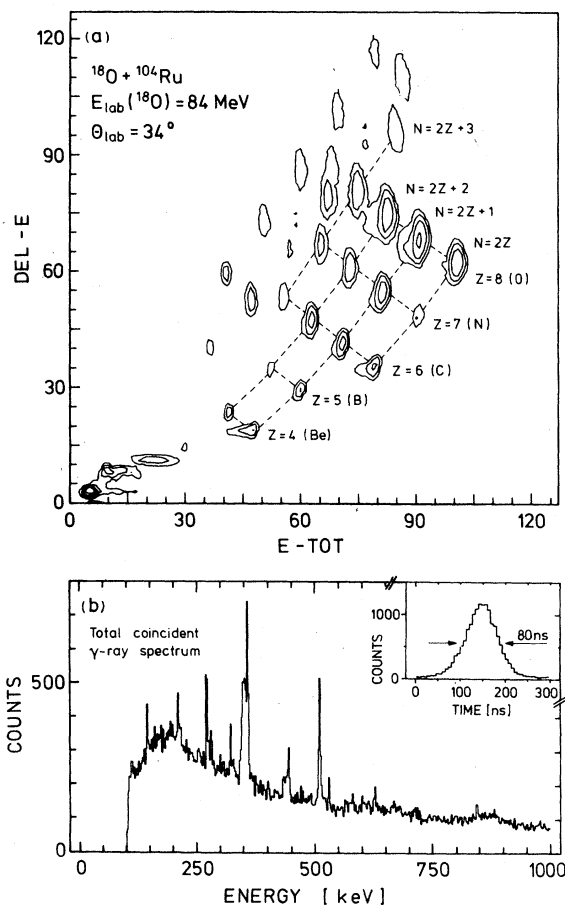


FIG. 2. (a) ΔE - E_{tot} spectrum obtained for the reaction $^{18}\text{O} + ^{104}\text{Ru}$. The labeled ejectile groups have maximum atomic charge state values. (b) Gamma-ray spectrum coincident with all particles shown in Fig. 2(a). The insert shows the time spectrum of ^{16}O - γ coincidences.

tive particle groups and on the corresponding prompt time peaks. The measured Q values were converted into excitation energies in the heavy final

TABLE I. Experimental conditions.

Target nucleus	Target thickness ($\mu\text{g}/\text{cm}^2$)	Isotopic enrichment (%)	E_{lab} (^{18}O) (MeV)	θ_{lab} (ejectiles) ($^\circ$)	L_{graz} ($\#$)
^{100}Mo	192	97.4	84	34	45
^{104}Ru	520 (on 34 $\mu\text{g}/\text{cm}^2$ C)	99	84	34	44
			100	30	55

nuclei by assuming that the light particles are emitted in their respective ground states. It is known for other asymmetric systems that in deep-inelastic reactions where particles are transferred to the heavy partner the ejectile excitation probability is small (≤ 0.25).¹³

A. $^{104}\text{Ru} (^{18}\text{O}, ^{16}\text{O})^{106}\text{Ru}$

Figure 3(a) shows a γ -ray spectrum for the reaction $^{104}\text{Ru} (^{18}\text{O}, ^{16}\text{O})^{106}\text{Ru}$ measured at 84 MeV incident energy, for excitation energies between 1.3–9.9 MeV in ^{106}Ru . Although many unresolved states are populated in this energy range, the γ decay from all these states results in a spectrum with very few individual lines. The occurrence of annihilation radiation (511 keV) indicates the importance of many unresolved higher energy γ transitions. The discrete γ transitions observed are summarized in Table II. In addition to γ transitions between known³ states with $I^\pi \leq 4^+$, two previously unobserved lines with energies 581.1 and 677.6 keV show up. In order to see from which regions within the E^* vs I plane (see Fig. 1) these γ transitions originate, the total excitation energy range was divided into three consecutive energy bins, each ~ 2.5 MeV wide. Spectra coincident to these sub-bins are shown in Fig. 3(b)–(d), and γ intensities relative to the 270 keV $2_1^+ - 0_1^+$ transition are given for each bin in Table II. For the lowest lying bin [Fig. 3(d)] only the $2_1^+ - 0_1^+$ and

$4_1^+ - 2_1^+$ transitions are visible, with an intensity ratio $N(4_1^+ - 2_1^+)/N(2_1^+ - 0_1^+) = (35 \pm 10)\%$, which is about 30 times larger than observed in β^- decay of ^{106}Tc ,³ demonstrating the advantage of using the heavy ion induced transfer reaction for the investigation of higher spin states in neutron rich nuclei. This intensity ratio increases with increasing excitation energy, yielding only a $\sim 30\%$ sidefeeding of the 2_1^+ level from states other than the 4^+ yrast state for the highest lying excitation energy bin [Fig. 3(b)]. This behavior can be understood because states with larger angular momenta are preferred at the higher lying excitation energy bins. A similar relative enhancement in γ -ray intensity with increasing excitation energy is evident from Table II for the newly observed 581.1 and 677.6 keV γ lines: The 581 keV γ transition clearly shows up first in the medium excitation energy bin [Fig. 3(c)] and strongly grows in intensity relative to the $2^+ - 0^+$ yrast transition by going to the highest bin. For the 678 keV transition there is only a hint in the medium bin, whereas it is clearly present in the highest bin. At this excitation energy range the relative strength for L transfer of $6\hbar$ is predicted by the DWBA calculations to have its maximum value and that of $L = 8\hbar$ transfer is rapidly growing. Therefore, it is highly suggestive to assign the 581 and 678 keV γ lines to the $6^+ - 4^+$ and $8^+ - 6^+$ yrast transitions in ^{106}Ru , respectively.

Two other levels in ^{106}Ru , i.e., 2_2^+ and 3_1^+ , also show a characteristic dependence of their popula-

TABLE II. γ -ray transitions in ^{106}Ru observed in the reaction $^{104}\text{Ru} (^{18}\text{O}, ^{16}\text{O})^{106}\text{Ru}$.

E_γ^a (keV)	Transition $I_i^\pi - I_f^\pi$	Relative intensity (%)		
		measured for excitation energy ranges		
		1.6–4.0 MeV	4.0–6.8 MeV	6.8–9.9 MeV
270.07(6)	$2_1^+ - 0_1^+$	100	100	100
444.7(1)	$4_1^+ - 2_1^+$	35 ± 10	40 ± 7	69 ± 10
581.1(2)	$(6_1^+ - 4_1^+)$		10 ± 4	29 ± 7
677.6(4)	$(8_1^+ - 6_1^+)$			12 ± 5
522.4(3)	$2_2^+ - 2_1^+$		15 ± 5	
792.0(7)	$2_2^+ - 0_1^+$		13 ± 5	
821.3(3)	$3_1^+ - 2_1^+$			22 ± 7

^aUncertainties in the least significant digit are given in parentheses.

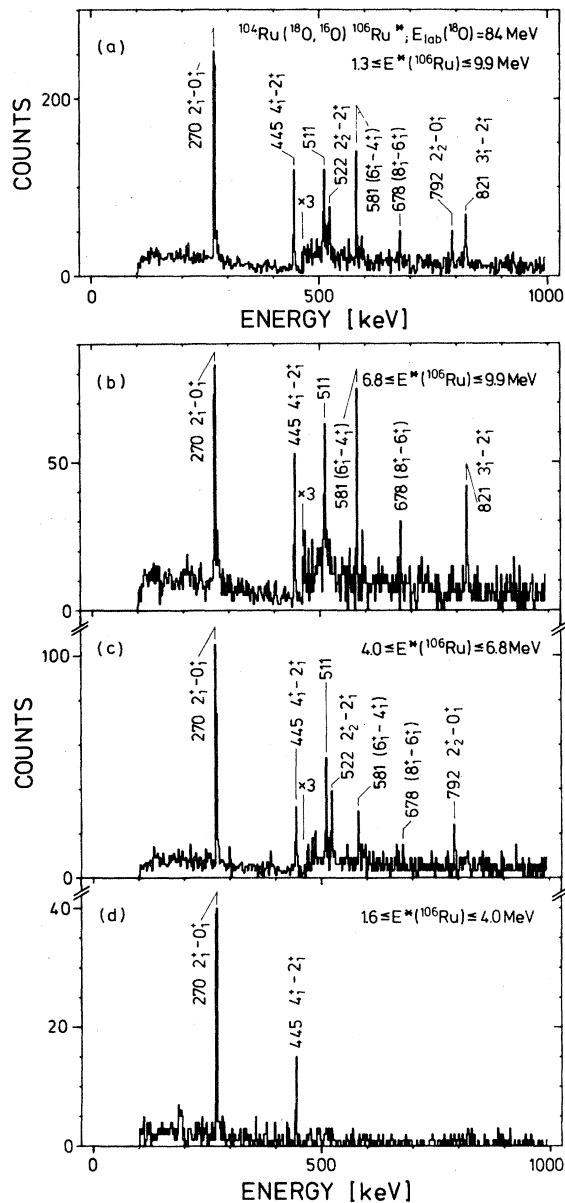


FIG. 3. Gamma-ray spectra coincident with ^{16}O ejectiles produced in the reaction $^{104}\text{Ru}(^{18}\text{O}, ^{16}\text{O})^{106}\text{Ru}$ for different excitation energy ranges in ^{106}Ru . (a) Total range (1.3–9.9 MeV), (b)–(d) subdivisions of total range: (b) 6.8–9.9 MeV, (c) 4.0–6.8 MeV, and (d) 1.6–4.0 MeV.

tion with changing excitation energy but displaced to the behavior observed for the members of the ground state band. As evident from Fig. 3, γ decay from both levels is not observed for the lowest lying bin, where γ decay from the 4^+ and 2^+ yrast states is clearly present. By comparing the γ -ray

spectra coincident to the upper two excitation energy bins [Figs. 3(b) and (c)] it can be seen that γ decay of the 3_1^+ level is almost restricted to the uppermost bin, whereas γ transitions from the 2_2^+ state occur more strongly in the medium bin. (It is known³ that the 3_1^+ level predominantly decays to the 2_1^+ level of the ground state band and not to the 2_2^+ state.) From comparison with less neutron rich even Ru isotopes these two levels may be thought of as being the lowest two members of a γ -vibrational band built on the 2_2^+ bandhead at 792 keV excitation energy. Thus also population intensities of states located in the vicinity of the yrast line, which very likely form an excited (collective) band with a different intrinsic structure, show an angular momentum selectivity similar to the one observed for the ground state band.

Figure 4 gives an example for a γ -ray spectrum coincident with ^{16}O ejectiles if the excitation energy window is positioned above (for $I=0$) the $\Gamma_\gamma \approx \Gamma_n$ line for ^{106}Ru ($10.9 \leq E^* \leq 16.1$ MeV). In this case the reaction was induced at 100 MeV incident energy and at a correspondingly smaller grazing angle. However, the qualitative features of the reaction as discussed in Sec. II are not expected to be much different. Compared to Fig. 3(b), where only γ decay from states in ^{106}Ru was observed, Fig. 4 now reveals a completely different γ -ray spectrum. New γ lines show up due to γ decay of states located in ^{105}Ru .

B. $^{100}\text{Mo}(^{18}\text{O}, ^{16}\text{O})^{102}\text{Mo}$

Figure 5 shows γ -ray spectra for the reaction $^{100}\text{Mo}(^{18}\text{O}, ^{16}\text{O})^{102}\text{Mo}$ at 84 MeV incident energy,

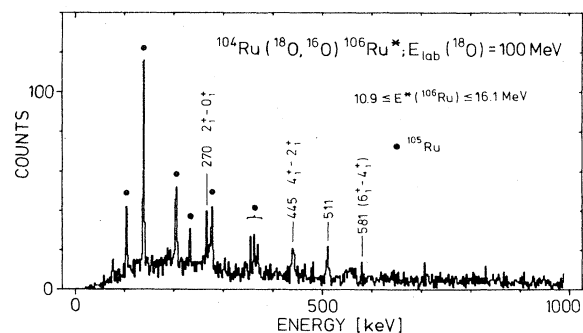


FIG. 4. Gamma-ray spectrum coincident with ^{16}O ejectiles produced in the reaction $^{104}\text{Ru}(^{18}\text{O}, ^{16}\text{O})^{106}\text{Ru}$ for the excitation energy range 10.9–16.1 MeV in ^{106}Ru . Gamma lines labeled by solid dots are due to transitions in ^{105}Ru .

coincident to three successive excitation energy bins, all centered below the one neutron binding energy (8.17 MeV) in ^{102}Mo . Similar to the case of ^{106}Ru (Sec. IV A) only a few γ transitions show up for each bin. These transitions together with their relative intensities are listed in Table III. A strong increase of the intensity of the $4^+ - 2^+$ transition relative to the $2^+ - 0^+$ yrast transition is observed for the higher lying excitation energy bins. This intensity ratio is much larger than obtained in a previous experiment, where the same reaction was studied at bombarding energies close to the Coulomb barrier⁶ due to the larger angular momentum transfer at higher bombarding energies. In addition to known^{2,6} γ transitions between states with $I^\pi \leq 4^+$, two hitherto unobserved γ lines with energies 584.2 and 655.6 keV show up with their intensities increasing for higher excitation energy bins. This behavior resembles the one observed for ^{106}Ru . Thus the 584 and 656 keV γ transitions are attributed to the decay of the 6^+ and 8^+ yrast states in ^{102}Mo , respectively.

An inspection of low lying excitation energy bins reveals that also the first excited 0_2^+ state at 697 keV excitation energy is populated with visible strength. For example, the 400.9 keV $0_2^+ - 2_1^+$ γ transition clearly shows up in Fig. 5(c). This behavior is contrasted by the ^{106}Ru data, where the γ decay of the 0_2^+ state at 991 keV excitation energy via the 720.6 keV $0_2^+ - 2_1^+$ transition was not observed [cf. Fig. 3(d)]. Since no change in the

global behavior of the transfer reaction mechanism is expected to take place for Mo and Ru and because many levels above the 0_2^+ state are populated in each case, the observed difference in 0_2^+ population suggests a different selectivity due to a different intrinsic structure of the 0_2^+ state in ^{102}Mo and ^{106}Ru , respectively. Differences in the structure of 0_2^+ and other 0^+ states may also be deduced from (t,p) data,^{4,5} where considerable differences in the distribution of 0^+ strength was observed between the neutron rich Mo and Ru isotopes.

V. DISCUSSION

A. ^{106}Ru

The assignment of the newly observed 581.1 and 677.6 keV γ lines as the $6^+ - 4^+$ and $8^+ - 6^+$ yrast transitions, respectively, is further supported by a comparison with existing level systematics known from neighboring Ru isotopes. Figure 6(a) shows a compilation of experimentally known yrast states for the even Ru isotopes with $100 \leq A \leq 112$.^{14,15} It can be seen that the proposed 6^+ and 8^+ yrast states in ^{106}Ru fit well into the systematics. Recently, theoretical calculations for low lying (collective) states in the even Ru isotopes have been performed¹⁶ within the framework of the proton-neutron interacting boson model (IBA-2). These calculations reproduce the experimental excitation

TABLE III. γ -ray transitions in ^{102}Mo observed in the reaction $^{100}\text{Mo}(^{18}\text{O}, ^{16}\text{O})^{102}\text{Mo}$.

E_γ^a (keV)	Transition $I_i^\pi - I_f^\pi$	Relative intensity (%)		
		measured for excitation energy ranges		
		1.4–3.7 MeV	5.1–8.0 MeV	6.5–9.6 MeV
296.15(5)	$2_1^+ - 0_1^+$	100	100	100
447.2(1)	$4_1^+ - 2_1^+$	13 ± 7	49 ± 6	53 ± 6
584.2(2)	$(6_1^+ - 4_1^+)$		12 ± 3	19 ± 4
655.6(5)	$(8_1^+ - 6_1^+)$			11 ± 3
400.9(3)	$0_2^+ - 2_1^+$	67 ± 18		
551.7(2)	$2_2^+ - 2_1^+$		14 ± 3	12 ± 3
847.6(4)	$2_2^+ - 0_1^+$		5 ± 3	8 ± 3

^aUncertainties in the least significant digit are given in parentheses.

energies for yrast states, especially for those with $I^\pi \leq 4^+$. For ^{106}Ru transition energies of 260 keV ($2^+ - 0^+$), 426 keV ($4^+ - 2^+$), 576 keV ($6^+ - 4^+$), and 716 keV ($8^+ - 6^+$) were calculated. These predictions agree well with the observed values.

B. ^{102}Mo

The experimentally available yrast level systematics for the even Mo isotopes with $96 \leq A \leq 106$ is shown in Fig. 6(b) and supports the assignment of the 584.2 and 655.6 keV γ lines as the $6^+ - 4^+$ and $8^+ - 6^+$ yrast transitions in ^{102}Mo , respectively. No theoretical calculations of level schemes for the more neutron rich Mo iso-

topes are presently available. In γ -decay studies of primary fission fragments¹ γ transitions of 562 and 652 keV were tentatively assigned to the $6^+ - 4^+$ and $8^+ - 6^+$ yrast transitions, respectively. However, these values are subject to uncertainties up to 50 keV (and are possibly just extrapolations derived from VMI systematics).

VI. SUMMARY

It is shown by the present data that particle- γ coincidence spectroscopy at bombarding energies well above the Coulomb barrier employing a magnetic spectrograph is a valuable tool for the investi-

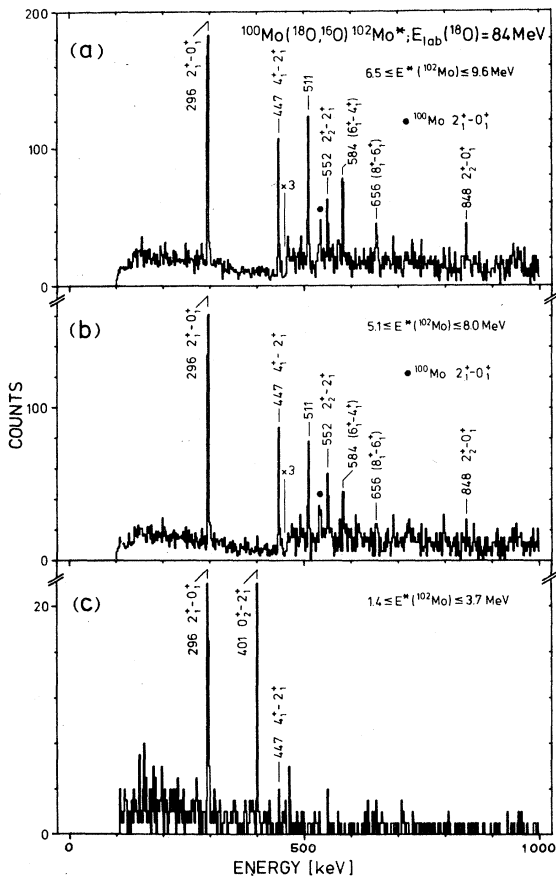


FIG. 5. Gamma-ray spectra coincident with ^{16}O ejectiles produced in the reaction $^{100}\text{Mo}(^{18}\text{O}, ^{16}\text{O})^{102}\text{Mo}$ for three different excitation energy ranges in ^{102}Mo : (a) 6.5 – 9.6 MeV, (b) 5.1 – 8.0 MeV, (c) 1.4 – 3.7 MeV. In (a) and (b) the solid dot marks the $2_1^+ - 0_1^+$ γ transition in ^{100}Mo due to the (^{18}O , ^{16}O) reaction on the target impurity ^{98}Mo .

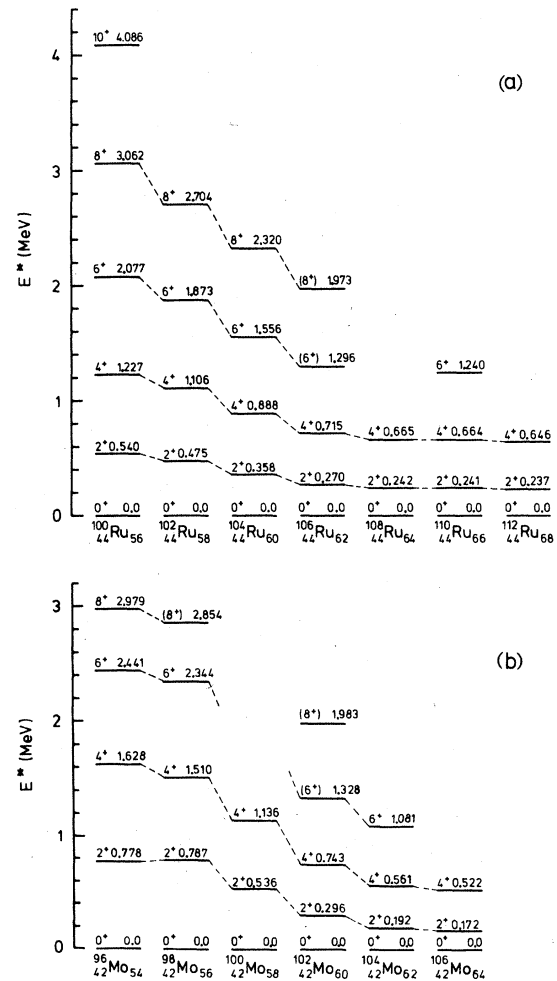


FIG. 6. Level systematics of experimentally known yrast states for (a) the even Ru and (b) the even Mo isotopes. For ^{106}Ru and ^{102}Mo the 6^+ and 8^+ yrast states are assigned from the present work.

gation of high spin states in neutron rich nuclei. This method can also be applied to other regions of the nuclidic chart, e.g., the region of well deformed rare earth nuclei, where information from fission product measurements is not available and where (t,p) reactions do not excite high spin states. Since the direct reactions represent only a small angular momentum window of the total reaction cross section it becomes possible with the method employed to investigate decay modes of selected regions in

the E^* vs I plane by changing the incident energy and the projectile-target combinations.

ACKNOWLEDGMENTS

We would like to thank Johanna Stachel for supplying us with the ^{104}Ru target. This work was supported by the Bundesministerium für Forschung und Technologie, Bonn, Federal Republic of Germany.

-
- ¹E. Cheifetz, J. B. Wilhelmy, R. C. Jared, and S. G. Thompson, Phys. Rev. C **4**, 1913 (1971).
- ²H. Ahrens, N. Kaffrell, N. Trautmann, and G. Herrmann, Phys. Rev. C **14**, 211 (1976).
- ³K. Sümmerer, N. Kaffrell, E. Stender, N. Trautmann, K. Brodén, G. Skarnemark, T. Björnstad, I. Haldorsen, and J. A. Maruhn, Nucl. Phys. **A339**, 74 (1980).
- ⁴R. F. Casten, E. R. Flynn, O. Hansen, and T. J. Mulligan, Nucl. Phys. **A184**, 357 (1972).
- ⁵E. R. Flynn, R. E. Brown, J. A. Cizewski, J. W. Sunier, W. P. Alford, E. Sugarbaker, and D. Ardouin, Phys. Rev. C **22**, 43 (1980).
- ⁶H. Bohn, P. Kienle, D. Proetel, and R. L. Hershberger, Z. Phys. A **274**, 327 (1975).
- ⁷H. Spieler, H. J. Körner, K. E. Rehm, M. Richter, and H. P. Rother, Z. Phys. A **278**, 241 (1976).
- ⁸W. Henning, Y. Eisen, H. J. Körner, D. G. Kovar, J. P. Schiffer, S. Vigdor, and B. Zeidman, Phys. Rev. C **17**, 2245 (1978).
- ⁹D. H. Gloeckner, M. H. Macfarlane, and S. C. Pieper, Argonne National Laboratory Report No. ANL-76-11, 1978 (unpublished).
- ¹⁰K. E. Rehm, H. J. Körner, M. Richter, H. P. Rother, J. P. Schiffer, and H. Spieler, Phys. Rev. C **12**, 1945 (1975).
- ¹¹W. A. Mayer, thesis, Technische Universität München, 1979 (unpublished).
- ¹²C. Chasman, S. Cochavi, M. J. LeVine, and A. Z. Schwarzschild, Phys. Rev. Lett. **28**, 843 (1972).
- ¹³H. Puchta, Ph. D. thesis, Universität München, 1979 (unpublished).
- ¹⁴J. Stachel, N. Kaffrell, H. Emling, H. Folger, E. Grosse, R. Kulesa, and D. Schwalm, GSI Annual Report 1980 (unpublished); J. Stachel (private communication).
- ¹⁵*Table of Isotopes*, 7th ed., edited by C. M. Lederer and V. S. Shirley (Wiley, New York, 1978).
- ¹⁶P. van Isacker and G. Puddu, Nucl. Phys. **A348**, 125 (1980); P. van Isacker (private communication).